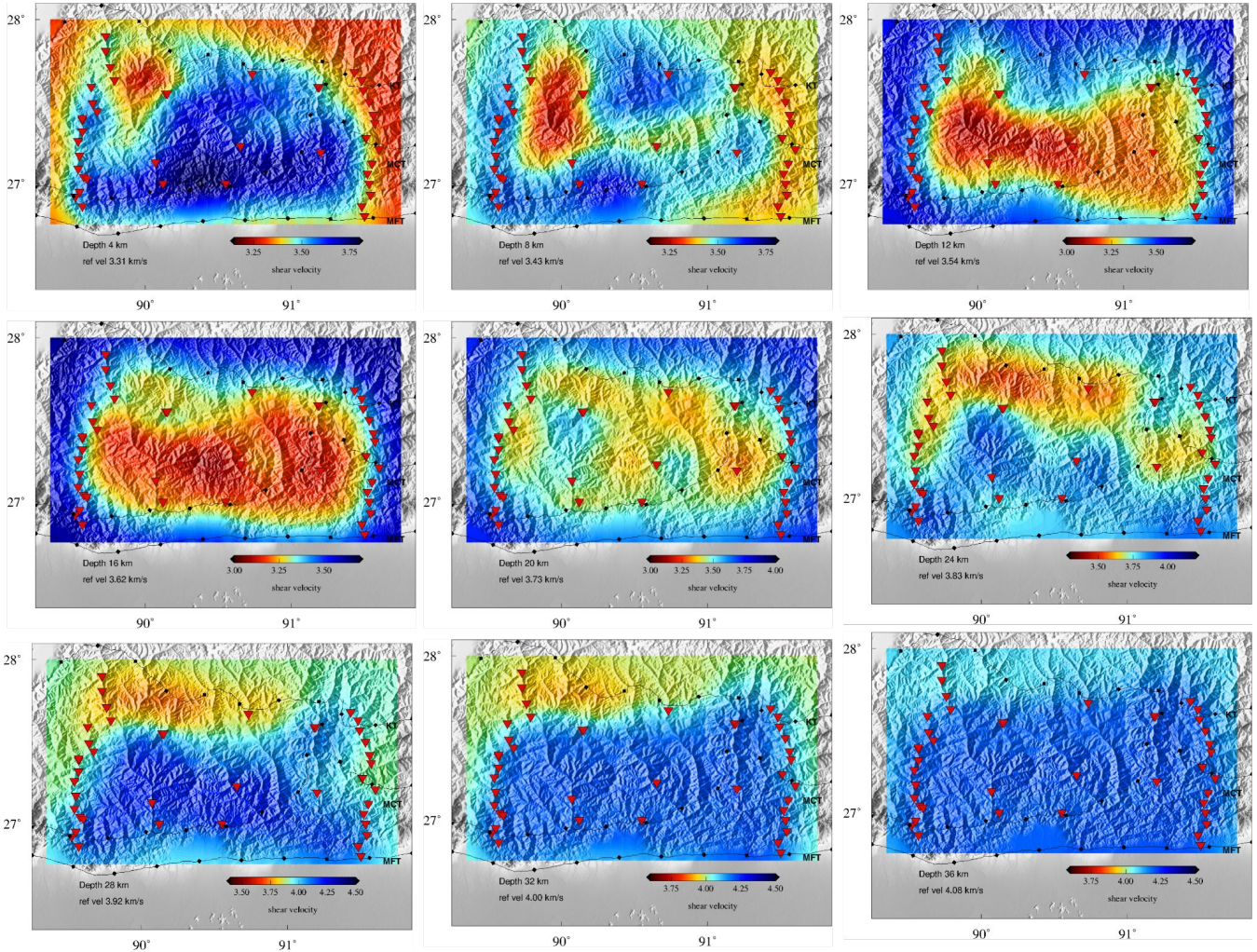

Figure S1: Shear wave velocity structure of the Bhutan Himalayas obtained using three-dimensional surface wave inversion. Each panel displays the horizontal cross-sections of the derived 3-D shear wave velocity models at different depths, as indicated in the lower left corner of each panel.

Gaurav Kumar
(gauravk20@iiserb.ac.in)

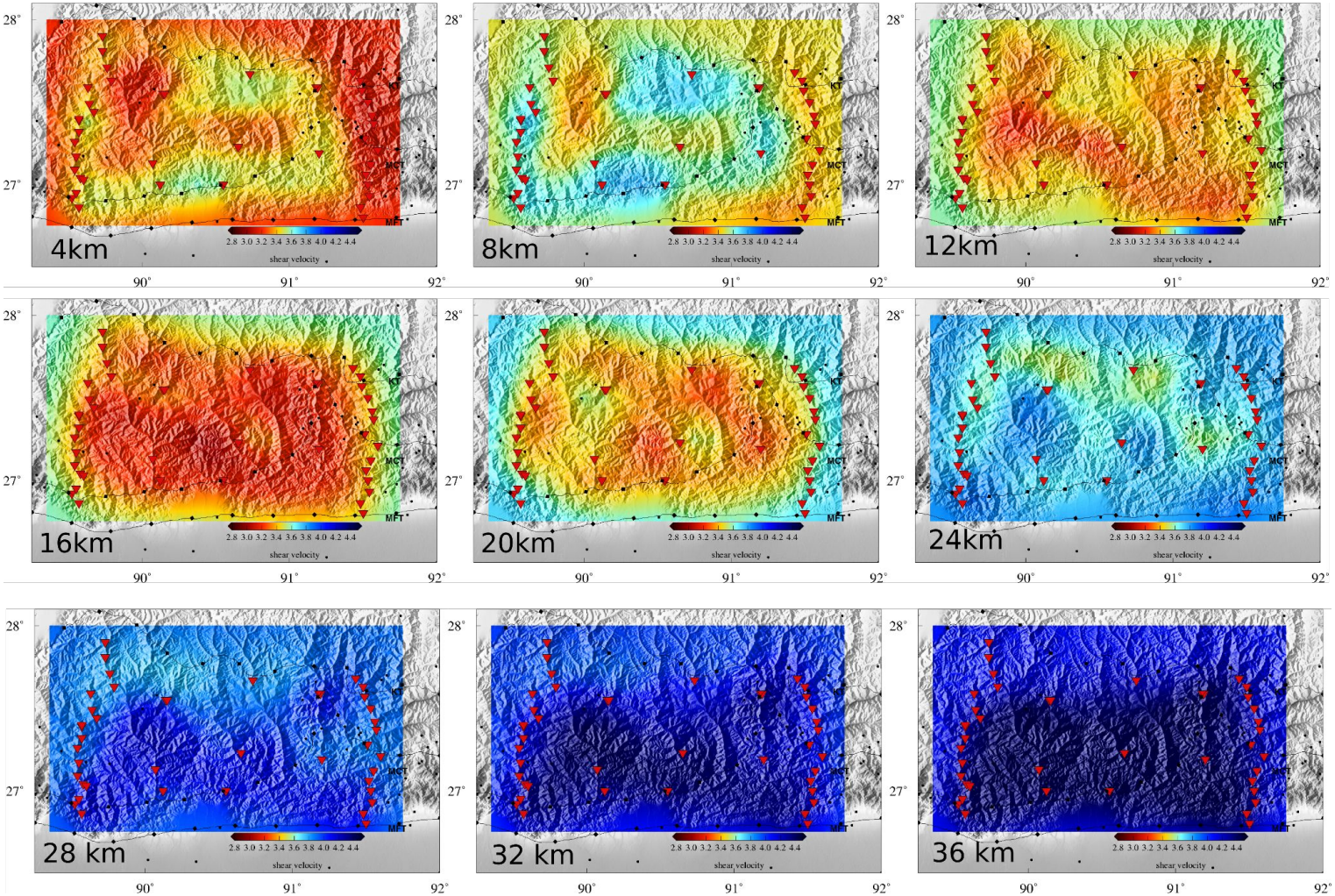

Figure S2: The figure illustrates the horizontal cross-sections of the derived 3-D shear wave velocity models at different depths, as indicated in the lower left panel of each section. The velocity variation in each panel at different depths is shown using a constant shear wave velocity scale ranging from a minimum of 2.8 km/s to 4.5 km/s.

Gaurav Kumar
(gauravk20@iiserb.ac.in)

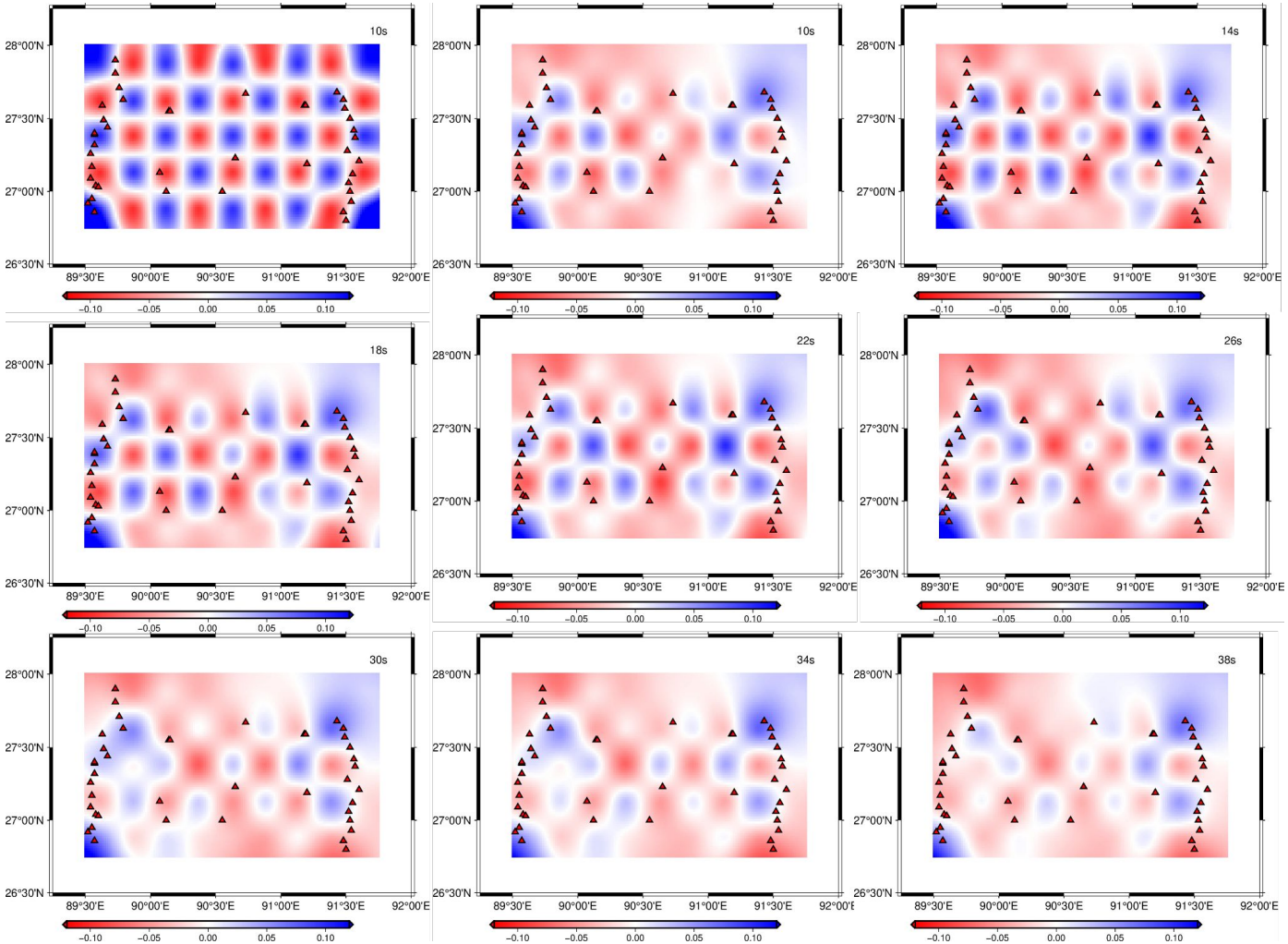

Figure S4: The map illustrates the synthetic checkerboard resolution test for various time periods, with a cell size of 0.25° x 0.25° and a damping value of 0.0002. The graphic in the upper left panel depicts a checkerboard synthetic model, while the graphics in the other panels illustrate the recovery model at 10 s, 14 s, 18 s, 22 s, 26 s, 30 s, 34 s, and 38 s time periods.

Gaurav Kumar
(gauravk20@iiserb.ac.in)

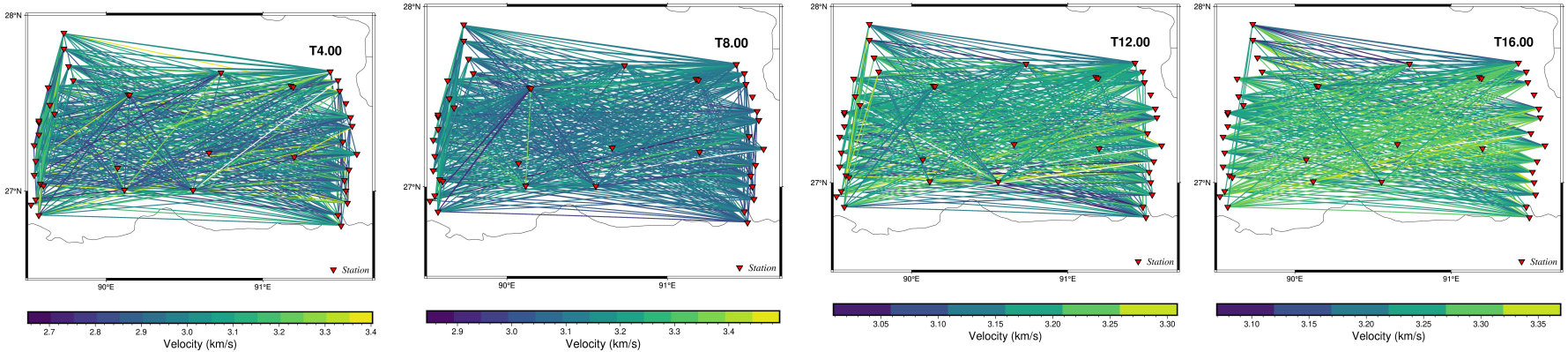

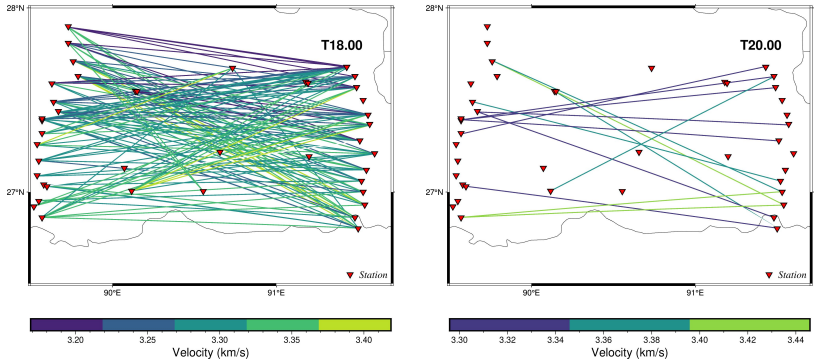

Figure S5: The map illustrates the ray path density for various time periods for the ANT method.

Gaurav Kumar
(gauravk20@iiserb.ac.in)

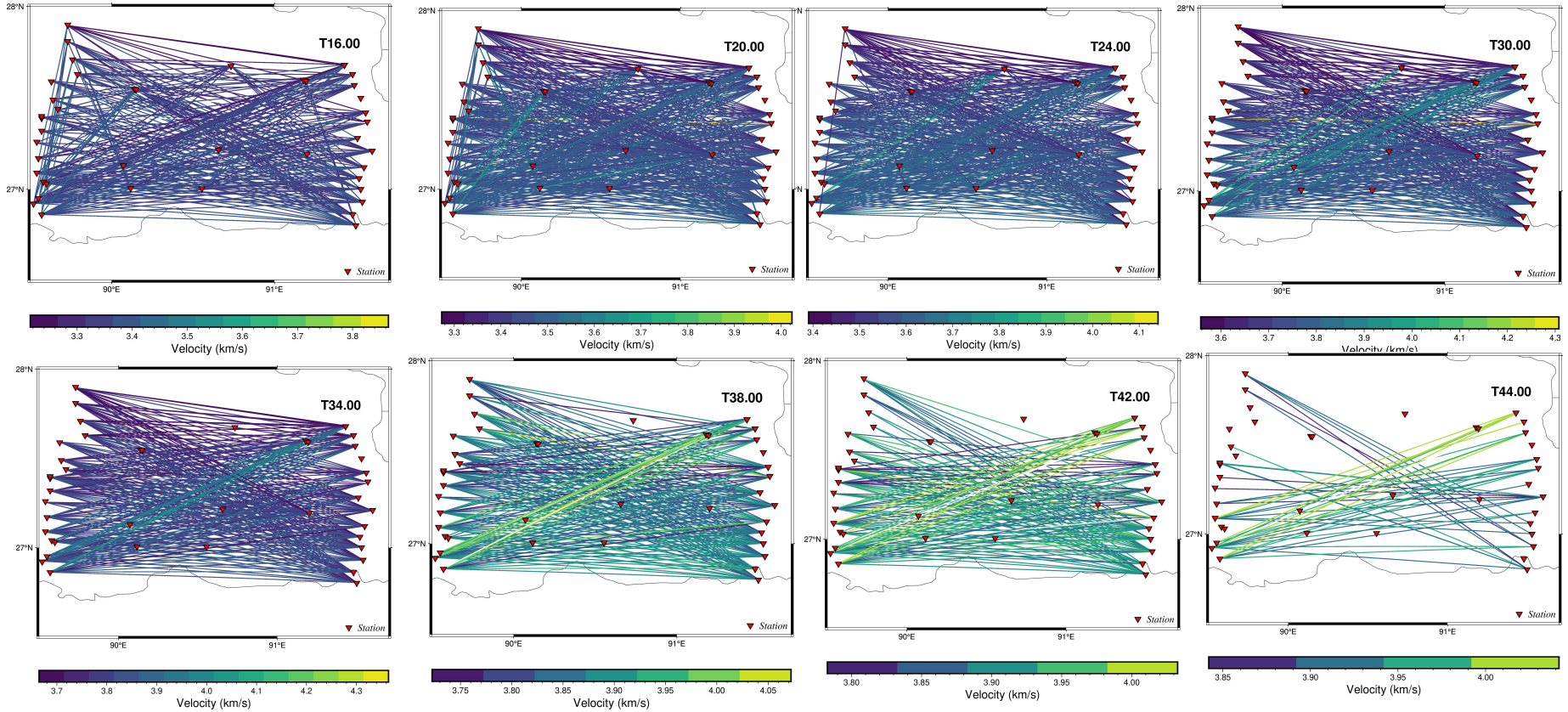

Figure S6: The map illustrates the ray path density for various time periods for the TSM method.

Gaurav Kumar
(gauravk20@iiserb.ac.in)

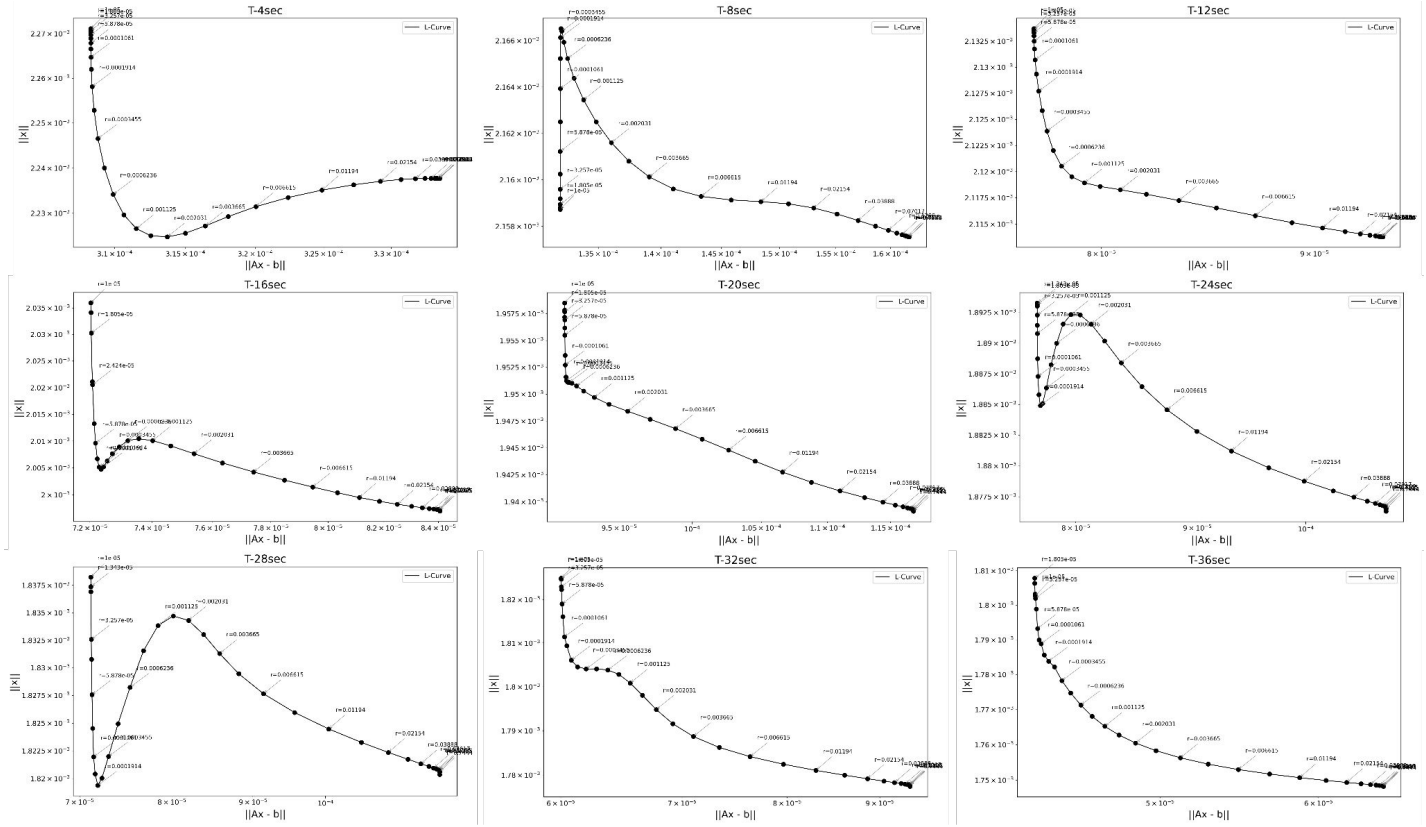

Figure S7: L curve plot of data misfit versus model misfit over various time periods (as shown in each panel of the image) for a cell size of 0.25. The x-axis denotes data misfit and the y-axis represents model misfit.

Gaurav Kumar
(gauravk20@iiserb.ac.in)

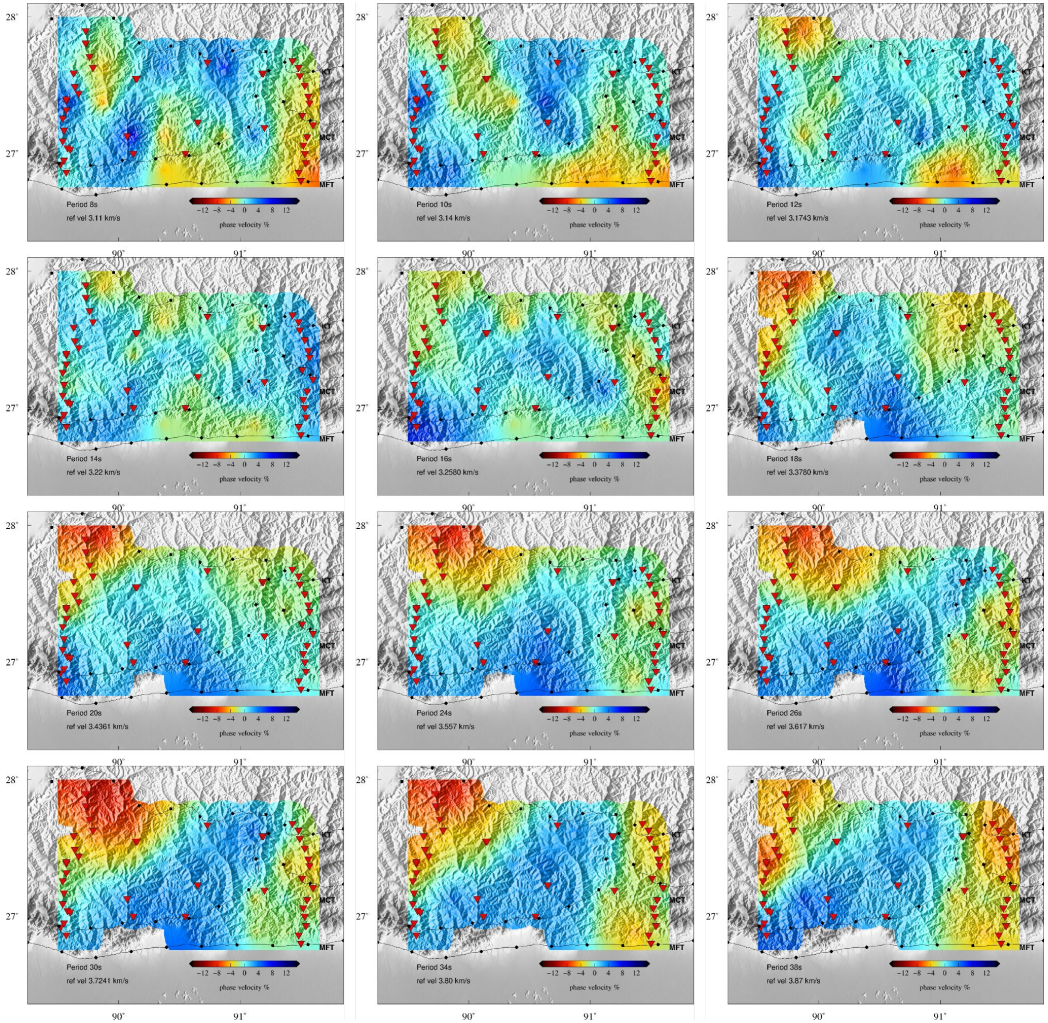

Figure S8: Anomaly maps of Rayleigh wave phase velocity derived from seismic tomography using ambient noise and teleseismic earthquake data, spanning from 8 s to 38 s, as specified in the lower-left corner of each panel. The velocity anomalies are computed relative to the average velocity of the study area, as indicated in the lower left corner of each panel.

Gaurav Kumar
(gauravk20@iiserb.ac.in)

Reference:

Julia Singer, Anne Obermann, Eduard Kissling, Hongjian Fang, György Hetényi,and Djordje Grujic. Along-strike variations in the Himalayan orogenic wedge structure in Bhutan from ambient seismic noise tomography. Geochemistry, Geophysics,Geosystems, 18(4):1483–1498, 2017.

Julia Singer, Edi Kissling, Tobias Diehl, and György Hetényi. The underthrusting Indian crust and its role in collision dynamics of the Eastern Himalaya in Bhutan: Insights from receiver function imaging. Journal of Geophysical Research: Solid Earth, 122(2):1152–1178, 2017. Wiley Online Library

Anne Obermann, Elmer Ruigrok, Irene Bianchi, and György Hetényi. Constraining the Moho depth below Bhutan with global-phase seismic interferometry. Frontiers in Earth Science, 9:658146, 2021.

Djordje Grujic, György Hetényi, Rodolphe Cattin, Saurabh Baruah, Angélique Benoit, Dowchu Drukpa, and Adi Saric. Stress transfer and connectivity between the Bhutan Himalaya and the Shillong Plateau. Tectonophysics, 744:322–332, 2018

R. A. Soomro, C. Weidle, L. Cristiano, S. Lebedev, T. Meier, and PASSEQ Working Group. Phase velocities of Rayleigh and Love waves in central and northern Europe from automated, broad-band, interstation measurements. Geophysical Journal International, 204(1):517–534, 2016.